Applied Nanoscience (2022) 12:3871–3882
https://doi.org/10.1007/s13204-022-02539-x

ORIGINAL ARTICLE

Effective treatment of resistant opportunistic fungi associated with immuno-compromised individuals using silver biosynthesized nanoparticles

Abobakr Almansob[1] · Ali H. Bahkali[1] · Ahmed Albarrag[2] · Mohammad Alshomrani[3] · Abdulwahab Binjomah[3] · Waleed A. Hailan[4] · Fuad Ameen[1]

Received: 19 April 2022 / Accepted: 3 June 2022 / Published online: 23 July 2022

Abstract

Drug resistance in filamentous fungus to antifungal medicines is a huge problem in biomedical applications; so, an effective strategy for treating opportunistic fungal infections is needed. *Mentha piperita* is a very fascinating plant to treat a variety of ailments as home remedies. Eighteen strains of *Aspergillus* species were used for this study which are having a unique antifungal resistance profile in presence of silver nanoparticles (AgNPs). AgNPs were prepared, using an aqueous extract of *M. Piperita* and characterized it by various techniques. Structural properties of AgNPs were systematically studied using X-ray diffraction (XRD), high-resolution transmission electron microscopy (HRTEM), Fourier-transform infrared spectroscopy (FT-IR), and Raman measurement, which emanate the single-phase fcc structure of silver nanoparticles. The spherical nature and elemental analysis of as-synthesized AgNPs were confirmed using scanning electron microscopy (SEM) and energy-dispersive X-ray (EDX) spectroscopy, respectively. The optical study has been analyzed using UV–Vis spectroscopy and band gap was calculated as 2.51 eV, using Tauc plot. To analyze and validate the good efficacy of the disc approach, antifungal activity of AgNPs nanoparticles in different concentrations against isolates was achieved in both disc and broth microdilution. The extracellular enzymatic activity of *A. fumigatus* was found to explore the precise impact of nanoparticles on fungal metabolism. The antifungal efficacy of AgNPs against all fungi was highly successful in disc method. The broth approach underlined the favorable results of the disc method. It provided more precise results in determining the minimum inhibition concentration (MIC), as well as the minimum effective concentration (MEC). *A. fumigatus* (AM6) enzymatic activity was boosted by AgNPs. Also, ß-galactosidase, ß-glucuronidase, and ß-glucosidase are necessary enzymes whose activity has been boosted. Consequently, *M. piperita* AgNPs can play a major and intriguing function against resistant *Aspergillus* species with a significant shift in the enzymatic activity profile of fungi due to this action.

Keywords *Aspergillus* · Silver nanoparticles · *Mentha piperita* · Enzymatic activity

Introduction

Opportunistic mycoses are major fungal diseases whose risk has recently been increased because of the alteration in the fungus physiology, host immunological status, or environmental circumstances (Gnat et al. 2021; Almansob et al. 2022). This significant condition is identified as a potentially fatal illness in immune-compromised individuals and, more recently, in COVID-19 pandemic, especially with aspergillosis (Song et al. 2020). *Aspergillus* species cause aspergillosis, namely, *Aspergillus fumigatus*, *Aspergillus niger*, *Aspergillus flavus*, and *Aspergillus terreus*, which are resulting in a variety of infections ranging from noninvasive to invasive

✉ Fuad Ameen
fuadameen@ksu.edu.sa

1 Department of Botany & Microbiology, College of Science, King Saud University, Riyadh 11451, Saudi Arabia

2 Department of Pathology, College of Medicine, King Saud University, Saudi Arabia, Riyadh 11451, Saudi Arabia

3 Department of Microbiology, Regional Laboratory and Blood Bank, Saudi Arabia, Riyadh 11451, Saudi Arabia

4 Department of Zoology, College of Science, King Saud University, P.O. Box 2455, Riyadh 11451, Saudi Arabia

(Siddiqi et al. 2018; Maddy et al. 2019; Rudramurthy et al. 2019).

Fungal infections have long been recognized in the Kingdom of Saudi Arabia. According to previous statistics, fungal infections account for around 31% of all infections with *Aspergillus,* which constituting 12.38% of all infections (Almahdi et al. 2016). Moreover, the fungal infections accounted for roughly 10%, bacterial infections (gram-positive organisms: 10% and gram-negative organisms: 32%) accounted for 42%, and polymicrobial infections accounted for the remaining 48%. (Almuneef et al. 2006; Al-Tawfiq and Abed 2009; Ameen et al. 2022). However, in Saudi Arabia, specific information on opportunistic fungal infection is scarce. Consequently, the opportunistic fungal infection related to immune-compromised individuals will be explored in this paper systematically. Also, the drug resistance of filamentous fungi to antifungal drugs is a big concern in the medical field (Arendrup 2014; Ameen 2022). So, an effective treatment method is required to medicate the opportunistic fungal infections. Surprisingly, the different nanoparticles (NPs) are gaining extensive use in various biological therapies such as antifungal and antibacterial activity (Sathishkumar et al. 2016a; Rajadurai et al. 2021). Several biological (using plant extract), chemical (sol–gel, auto-combustion, co-precipitation, hydrothermal, etc.) and physical approaches have been proposed to synthesize these nanoparticles such as Cu NPs (Usman et al. 2012), Au NPs (MubarakAli et al. 2011; Almansob et al. 2022), and Ag NPs (Sajjad et al. 2019; Khan et al. 2020a). But, the silver nanoparticles, synthesized by biological methods, employing microbes, enzymes, amino acids, proteins, and plant extracts, are shown to be more biocompatible, eco-friendly, cost-effective, and readily manufactured on a large industrial scale (Jadhav et al. 2016; Parlinska-Wojtan et al. 2016; Ameen et al. 2020). The *green synthesis* of nanoparticles using the plant extract, in particular, is a successful strategy that has widespread applicability in modern medicine (Inbathamizh et al. 2013; Sathishkumar et al. 2016b). Again, phytochemicals that are included in plant extracts function as a both reducing and stabilizing agents in creating nanoparticles. Conventionally, several plant components, such as *Mentha* species, have been used as natural biomedicine to treat various ailments such as respiratory issues, spasms, pain, gastrointestinal complaints, eye infections, bronchitis, gout, and giddiness (Sreelatha et al. 2009; Desam et al. 2019). So, these *Mentha* species will be very beneficial to synthesize the biocompatible Ag NPs, because these are themselves having the natural biomedicine properties.

In this report, the fungal pathogens linked with immune-compromised individuals were isolated and identified in this study. Also, the silver nanoparticles were produced from aqueous extract of *Mentha piperita* and characterized using various techniques such as XRD, FT-IR, TEM, Raman, SEM, EDX, and UV–Vis spectroscopy. This extract of *Mentha piperita* has historically been used to cure infection in home remedies, to develop nano-biomedicine for the treatment of fungal diseases.

Materials and methods

Collection and identification of fungi

The fungal isolates were obtained from the departments of King Khalid University Hospital and King Saud Medical City hospital in accordance with the Ministry of Health-Kingdom of Saudi Arabia (MOH-KSA) guidelines and following approval by the Institutional Review Board of King Khalid University Hospital in Research Project No. E-18–3066 (Almansob et al. 2022).

Plant materials

Well-grown *Mentha piperita* was collected from the supermarket and identified by Government Botanical Survey. The leaves of the plant were used for extract preparation.

Preparation of plant extract

The leaves of *M. piperita* were obtained and identified by the Government Botanical Survey, and the voucher specimen was kept. The plant leaves were dried for 7 days at 25℃ in an incubator (Memmert GmbH, Burladingen, Germany). To eliminate any surface pollutants, the dried leaves were ground (ALSAIF ELEC grinder, 90,582) and carefully rinsed with double-distilled water. The aqueous extract was prepared using the decoction extraction procedure. The extract was made in a precise 1:16 ratio (plant to solvent). In 160 mL of double-distilled water, 10 g of powdered material was dissolved. Overall, the extract concentration was 0.06 g/mL (62.5 mg/mL or 62,500 ppm). The extracts were placed in an incubator shaker (Gallenkamp, Gillingham, UK) and maintained at 25℃ overnight. Later, the extract was filtered in two stages using sterile big 124 cm filter sheets (Whatman type No. 1, Gillingham, UK) and Acrodisc Syringe Filters (0.45 m pore size/ Pall, New York, NY, USA) to remove any potential contamination (Almansob et al. 2022).

Biosynthesis of silver nanoparticles

The aqueous plant extract was mixed with 1 mM of aqueous solution of $AgNO_3$ (Nexgen Chemicl, India) in ratios (1:1, 1:5, 1:10, and 1:15) with small-scale volumes (1:1, 1:5, 1:10, and 1 ml:15 ml) in 20 ml sterile glass tubes. Incubation was applied at room temperature till the brownish color was formed. Then, large-scale volumes of plant extract

were achieved to prepare sufficient amount of nanoparticles (50 ml: 500 ml, and 50 ml:750 ml). Control was done in the same test procedures, ratio and conditions but sterilized DW with extracts was applied instead of $AgNO_3$ (Rajadurai et al. 2021).

The green biosynthesized of AgNPs were confirmed by UV–visible spectrophotometer and distilled water will be used as reference. The brownish solutions were centrifuged for 5–10 min/6000 − 1000 rpm (Heraeus Sepatech Labofuge A & MiniSpin Centrifuge, Germany) many times and subsequently washed twice with sterilized distilled water (DW) and Milli-Q water and one time with 90% ethanol to remove the excess Ag^+ ions and pigments. Then, the sediments were dried in an incubator (Memmert, Germany) for 24 h at 48–50 °C (Kim et al. 2018; Rajkumar et al. 2021).

Preparation of AgNPs stock solution

According to further experiments, nanoparticles were prepared in an aqueous solution to form antifungal activity. The stock concentration of each AgNPs were 1000 ppm and serial dilutions of this stock were done to get solutions with concentration 200 ppm,100 ppm,50 ppm and 25 ppm.

Characterization of AgNPs

The structural properties of AgNPs samples were evaluated using X-ray diffraction (XRD), transmission electron microscope (TEM), high-resolution transmittance electron microscope (HRTEM), selected-area electron diffraction (SAED), Fourier-transform infrared (FT-IR) spectroscopy, and Raman measurements. XRD measurement of AgNPs was performed on Shimadzu Lab XRD-6100 using Cu-Kα radiation ($\lambda = 1.54$ Å) at room temperature to check the phase purity and to determine crystal symmetry. TEM images were recorded at 200 kV using JEM 1011 Japan. FT-IR spectra were carried out using Perkin Elmer Spectrum-2. Raman spectroscopy has been carried out using Jobin Yvon Horibra LABRAM-HR with 473 nm laser light. Morphological measurement was done using SEM (JEOL, Japan) with energy-dispersive X-ray (EDX). UV–Vis absorbance spectra and band gap analysis had been studied using UV–Vis Spectrophotometer (JASCO, USA).

Antifungal activity of AgNPs

AgNPs solutions with varying concentrations (25, 50, 100, 200, and 1000 ppm) were produced, and 10 µL of the solutions was put onto the sterile discs. The antifungal activity was expressed as a zone of inhibition in millimeters (mean ± SD). As a reference method, the broth microdilution technique was used in accordance with the CLSI M38-A protocol to test the accuracy and sensitivity of the disc diffusion method (Almansob et al. 2022).

Effect of silver nanoparticles on extracellular fungal enzymes

Efficient silver nanoparticles against fungi were selected and studied its impact on the enzymatic activity of fungi. These fungi were selected due to their high cytotoxicity feature and their significant role in respiratory tract infection and complication in immune-compromised patients (Gutarowska et al. 2014). Nineteen extracellular enzymes profiling were investigated throughout the APIZYM (Biomeruex, France) strips test. The protocol is based on same protocol of Almansob et al. (2022) (Almansob et al. 2022).

Statistical analysis

All experiments were performed in triplicate and discribed as mean ± SD. Two-way ANOVA analysis was applied for designed experiment. $p < 0.05$ was checked for significance.

Results and discussion

Identification of isolates

Eighteen isolates provided from the source departments were revived, sub-cultured on Sabouraud's agar (Oxoid Ltd, Basingstoke) and incubated for 5 days at 28 °C. The pure cultures were stored in glycerol at -80 °C for further analysis. After morphological identification, fungal isolated cultures were molecularly characterized by partially sequencing 18S rRNA gene using universal primers ITS1 and ITS4 (Almansob et al. 2022). The sequences were processed using BioEdit software 7.2.4. For similarity search, the BLASTn search tool of NCBI was used. The processed sequences for fungal strains were submitted to the GenBank database and accession numbers were provided (Table 1).

Biosynthesis of silver nanoparticles

AgNPs formation was visually recorded depending on the brownish color formation, as shown in Fig. 1. During 4 h, Ratio 1:15 (extract $AgNO_3$) was the most active biosynthesis for AgNPs. Principle of nanoparticle formation from plant source based on presence of phytochemicals such as phenol, flavonoid, isoeugenol and spathulenol existing in *Mentha* leaves act as reducing agent converting element solution to metallic form (Jha et al. 2009; Ebrahimabadi et al. 2010; Jafarizad et al. 2015).

Table 1 List of isolated fungi and their Genbank accession numbers

No	Fungi and (strain)	NCBI Accession no	Similarity%	Practical code
1	*Aspergillus flavus* (AM1)	OK396684	100%	1.1
2	*A. flavus* (AM2)	OK396685	100%	1.2
3	*A. flavus* (AM3)	OK396686	100%	1.3
4	*A. flavus* (AM4)	OK396687	100%	1.4
5	*Aspergillus flavus* (AM5)	OK396688	100%	1.5
6	*Aspergillus fumigatus* (AM6)	OK396689	100%	2.1
7	*Aspergillus fumigatus* (AM7)	OK396690	100%	2.2
8	*Aspergillus niger* (AM8)	OK396691	100%	3.1
9	*Aspergillus niger (*AM9)	OK396692	100%	3.2
10	*Aspergillus terreus* (AM10)	OK396693	100%	4
11	*Aspergillus flavus* (AM11)	OK396694	100%	5
12	*Aspergillus flavus* (AM12)	OK396695	100%	6
13	*Aspergillus flavus* (AM13)	OK396696	100%	7
14	*Aspergillus terreus* 8	–	–	8
15	*Aspergillus flavus* (AM14)	OK396697	100%	9
16	*Aspergillus flavus* (AM15)	OK396698	100%	10
17	*Aspergillus flavus* (AM16)	OK396699	100%	11
18	*Aspergillus niger* (AM17)	OK396700	100%	12

Table 2 Efficacy of different concentrations of AgNPs of *Mentha piperita* against tested fungi (Disc technique)

No	Fungi	Inhibition zone (mm)				
		AgNPs				
		25	50	100	200	1000
1	*A. flavus (AM1)*	0 ± 0	0 ± 0	8.3 ± 0.6	9.7 ± 0.6	11.3 ± 0.6
2	*A. flavus (AM2)*	0 ± 0	0 ± 0	0 ± 0	6.3 ± 0.6	6.7 ± 0.6
3	*A. flavus (AM3)*	0 ± 0	0 ± 0	0 ± 0	7.7 ± 0.6	8 ± 1
4	*A. flavus (AM4)*	8.3 ± 0.6	9.3 ± 0.6	10.3 ± 0.6	11.3 ± 1.2	12.3 ± 1.2
5	*A. flavus (AM5)*	6.7 ± 0.6	7.3 ± 1.5	9 ± 2	9.7 ± 1.5	12.7 ± 0.6
6	*A. fumigatus (AM6)*	0 ± 0	0 ± 0	8.7 ± 0.6	9.7 ± 0.6	11.7 ± 0.6
7	A. *fumigatus (AM7)*	0 ± 0	0 ± 0	0 ± 0	0 ± 0	9.7 ± 0.6
8	A. *niger (AM8)*	0 ± 0	0 ± 0	0 ± 0	0 ± 0	10.7 ± 0.6
9	*A. niger (AM9)*	0 ± 0	0 ± 0	0 ± 0	9.3 ± 0.6	12.3 ± 0.6
10	*A. terreus (AM10)*	0 ± 0	0 ± 0	0 ± 0	6.3 ± 0.6	9.7 ± 0.6
11	*A. flavus (AM11)*	6.7 ± 0.6	7.7 ± 0.6	8.0 ± 0	8.0 ± 0	10.3 ± 0.6
12	A. *flavus (AM12)*	0 ± 0	0 ± 0	0 ± 0	0 ± 0	7.3 ± 0.6
13	A. *flavus (AM13)*	0 ± 0	0 ± 0	0 ± 0	0 ± 0	7.3 ± 0.6
14	*A. terreus 8*	0 ± 0	0 ± 0	6 ± 0	6.7 ± 0.6	8.3 ± 0.6
15	A. *flavus (AM14)*	0 ± 0	0 ± 0	0 ± 0	0 ± 0	6.3 ± 0.6
16	A. *flavus (AM15)*	0 ± 0	0 ± 0	0 ± 0	0 ± 0	9.7 ± 1.5
17	*A. flavus (AM16)*	6.7 ± 0.6	7.7 ± 0.6	9.3 ± 0.6	9.7 ± 0.6	10.7 ± 0.6
18	*A. niger (AM17)*	9.3 ± 1.5	9.7 ± 0.6	12.0 ± 1	12.3 ± 1.2	14.3 ± 1.2

Characterization of AgNPs

XRD

The XRD spectrum is recorded to investigate the crystal structure of biosynthesized silver nanoparticles to confirm the phase purity and single phase of the sample as represented in the Fig. 2. This XRD results are in good agreement as the values for a face centered cubic (fcc) structure of silver and it is operated in 2θ geometry. The diffraction peaks

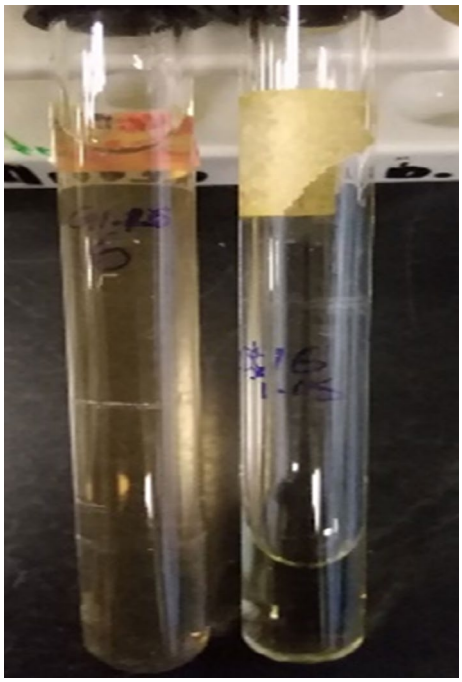

Fig. 1 AgNPs formation using *Mentha piperita* (1 min-4 h)

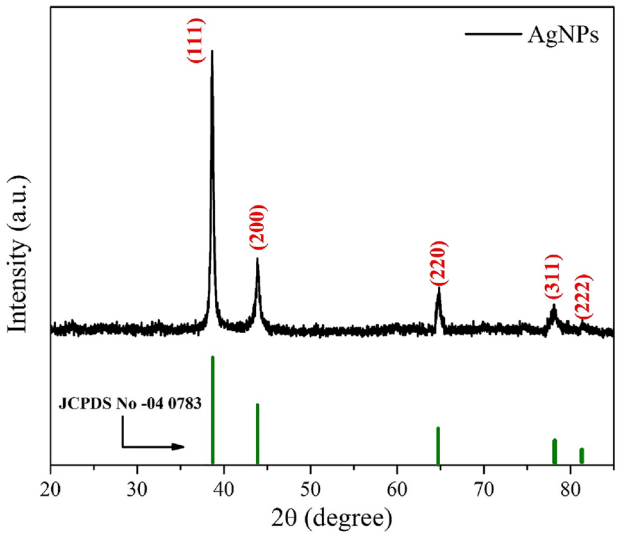

Fig. 2 XRD spectrum of AgNPs using *Mentha piperita* with JCPDS spectrum (04–0783)

observed at 38.6°, 43.8°, 64.7°, 78° and 81.1° correspond to the respective (111), (200), (220), (311), and (222) diffraction planes belonging to fcc structure of AgNPs, which is well matched with the JCPDS card number 04–0783 (Cai et al. 2017). The particles with sufficient energy orient along a thermodynamically favorable direction (111) and they move more actively towards thermodynamically stable sites in the Ag matrix. The calculated value of inter-planer spacing d accorded exactly with cubic structure of JCPDS card number 04-0783. No secondary peaks belonging to additional phase viz. Ag_2O structure were observed, which depicted the single-phase structure of AgNPs (MubarakAli et al. 2011). The fcc lattice parameter (a) of AgNPs is computed using the following expression (Eq. 1):

$$\frac{1}{d^2} = \frac{h^2 + k^2 + l^2}{a^2}, \tag{1}$$

where d is the interplanar spacing, calculated using the Bragg's formula (Eq. 2), and (hkl) is the Miller indices of each diffraction planes.

$$2dsin\theta = \lambda, \tag{2}$$

where λ is the wavelength of Cu Kα source of X-rays, and the value of θ is taken by the Gaussian curve fitting of (111) peaks. The value of lattice parameter is calculated to be 4.083 Å. Again, the average crystallite size (δ) was evaluated from the XRD analysis using Debye–Scherrer formulation (Khan et al. 2020b), as expressed by Eq. 3,

$$\delta = \frac{0.9\lambda}{\beta cos\theta}, \tag{3}$$

where β is the full width at half maxima of each peak and calculated value of average crystallite size (δ) was observed to be *22 nm* which has good agreement as the results obtained from the TEM analysis as mentioned in the Fig. 3 (a, b) (Abd Kelkawi et al. 2017; Kim et al. 2018).

TEM

Transmission electron microscopy (TEM), high-resolution transmission electron microscopy (HRTEM), and selected-area electron diffraction (SAED) observations were measured to study the greater vision of the morphology (particle distribution, and their size), fringe patterns of lattice and ring arrangements of the biologically synthesized AgNPs as shown in Fig. 3a. TEM image verified the spherical geometry with some clusters or agglomeration of silver nanocrystallites. Agglomeration of crystallites, and particles is a general activity that emanates in a decrease of surface free energy by enhancing their shape and decreasing the surface area. The agglomeration and accumulation of nanocrystalline materials is because of the adhesion of the particles through weak forces resulting to submicron sized structure (Roselina and Azizan 2012). The average particle size, calculated using image j software, is 30 nm with 15.4 nm standard deviation (SD). The particle size distribution, fitted by the Gauss curve fitting formulation is represented in Fig. 3b, which has good concurrence with the results obtained from XRD analysis.

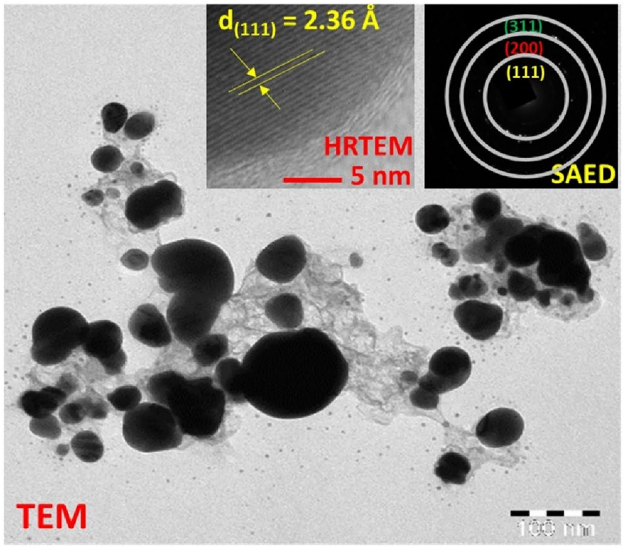

(a)

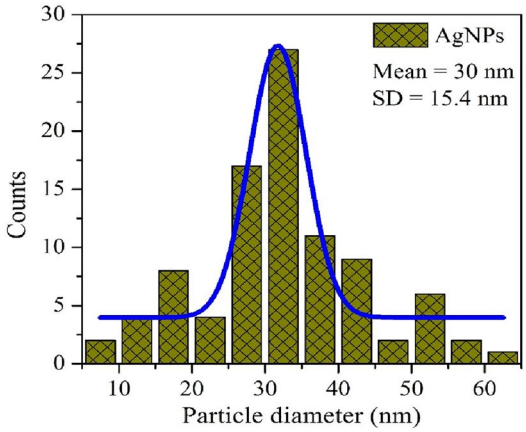

(b)

Fig. 3 TEM micrograph (**a**): insets show the corresponding HRTEM fringe pattern and SAED ring pattern, and particle size distribution using Gaussian curve fitting (**b**) of AgNPs

The HRTEM fringe pattern of lattice at very large magnification (scale: 5 nm) of biosynthesized nanoparticles has been analyzed in the first inset of Fig. 3a. The d-spacing had been measured to be 2.36 Å which indicates the (111) Miller plane of AgNPs (MubarakAli et al. 2011). Also, the SAED pattern investigated in the second inset of Fig. 3a exhibits rings network, emanating the nanoparticles polycrystalline behavior of pure AgNPs. Also, the d-spacing and corresponding plane observed from the HRTEM and SAED patterns could be well described to the fcc structure of AgNPs (Gabriela et al. 2017).

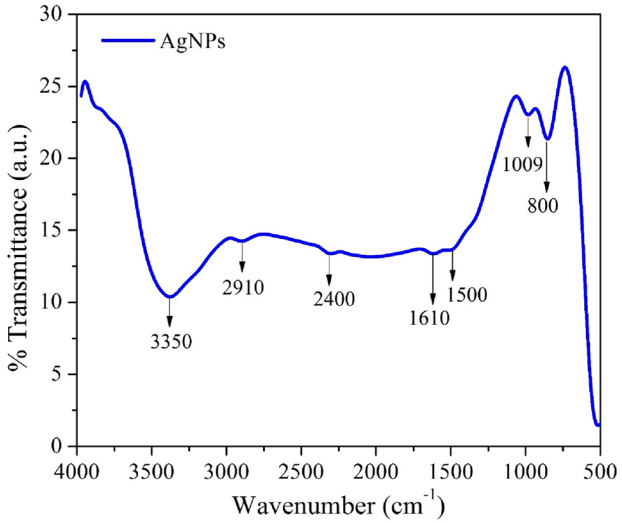

Fig. 4 FT-IR spectrum of AgNPs using *Mentha piperita*

FT-IR

The outcomes from FT-IR measurement described in Fig. 4 confirm the formation of the silver nanoparticles. The vibration bands, positioned below 1000 cm^{-1}, are called the finger print region in this spectrum AgNPs (Khan et al. 2020b). The stretching vibration of O–H bonds at 3350 cm^{-1} is obtained because of the moisture present in the sample (Khan and Rahman 2019). Our FTIR results indicated that the C–H vibration bond at 2910 cm^{-1} and strong stretching vibrations of O–H at 2400 cm^{-1}. Another two peaks at 1610 cm^{-1} and 1500 cm^{-1} attributed to the C=C stretching vibrations from the aromatic rings. Again, the peaks observed at 1009 cm^{-1} correspond to C–O stretching vibrations from alcohol, i.e., owing to functional groups of proteins and metabolites covering the silver nanoparticles. At last, the peak positioned at 800 cm^{-1} corresponds to the aromatic groups (Thirunavoukkarasu et al. 2013).

Raman

Raman spectrum of silver nanoparticles is shown in Fig. 5. It consists of vibrational modes at 233 cm^{-1}, 470 cm^{-1}, 627 cm^{-1}, and 1080 cm^{-1}. Well-formed silver nanoparticles were prepared using *Mentha piperita* extract which also play a vital role as a surfactant for AgNPs. The plant extract contained of several organic constituents like hydroxyl and carboxylic group. In the typical Raman spectrum, the band observed at 233 cm^{-1} corresponds to Ag–O stretching vibrational mode (Linic et al. 2015), further, the vibrational peaks positioned at 470 cm^{-1} and 627 cm^{-1} are created due to stretching vibration of C–N–C and C–S–C (Arvizo et al. 2012). The last band at 1080 cm^{-1} is obtained due to the

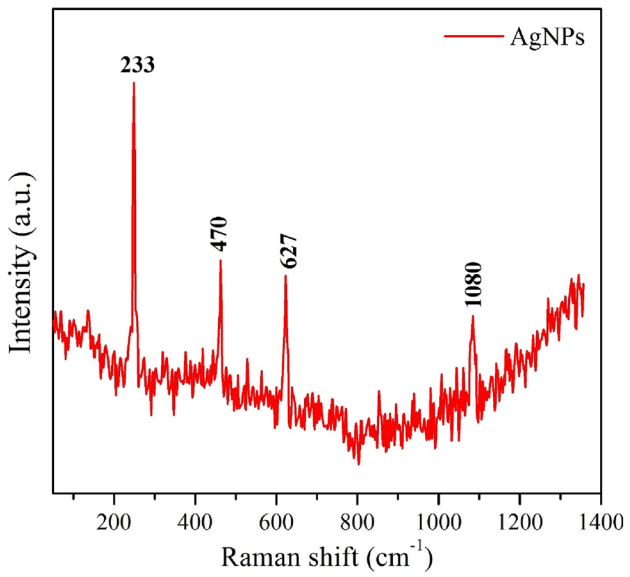

Fig. 5 Raman spectrum of AgNPs using *Mentha piperita*

carboxylic group (C = O stretching vibration) (Joshi et al. 2018).

SEM–EDX

The morphology and elemental analysis of AgNPs powder had been investigated using SEM and EDX, respectively. The SEM measurement was utilized to study the surface topography and morphology of the biosynthesized AgNPs, as represented in the inset of Fig. 6, which emanates the spherical shape with flat structure of the AgNPs (Habibi et al. 2010). These as-synthesized nanoparticles also formed some specific clusters in spite of close symmetry. Moreover, the NPs are apprehended by each other by *M. piperita* (stabilizing agent), which plays a vital role in managing the dispensation of particle size and also controlling the some specific aggregation (Feng et al. 2012). This particular observation that the plant extract of *Mentha piperita* is a proper capping agent, exhibits in creation of small sized nanoparticles. On the other hand, EDX spectroscopy attached with SEM microscope is used to recognize the elemental configuration of the biosynthesized AgNPs. The observed EDX spectrum of AgNPs is well represented in the Fig. 6, addressing the confirmation of silver (Ag), oxygen (O) and carbon (C) at their corresponding energy value. The observed spectrum of AgNPs is similar as previously reported study (Khan et al. 2016; Murugesan et al. 2017), rather to observe slightly spiked peak of carbon. The O and C peaks confirmed the presence of carbon-based stabilizers in the sample. Moreover, the presence of the C and O elements may correspond to the carbon tape utilized to mount the desired sample during the experiment and oxidation of surface, respectively (Abdul et al. 2011).

UV–Vis spectroscopy

UV–Vis spectroscopy is one of the important tools and techniques to study the optical properties of the different nanomaterials. As a multifaceted and having excellent application in various fields, the optical property of AgNPs sample needs to be investigated systematically. To measure the optical absorbance spectra of the AgNPs and plant extract were performed with a UV–Vis double beam spectrophotometer as shown in Fig. 7a, b. The typical absorbance spectra of both the samples show that the large absorption is obtained

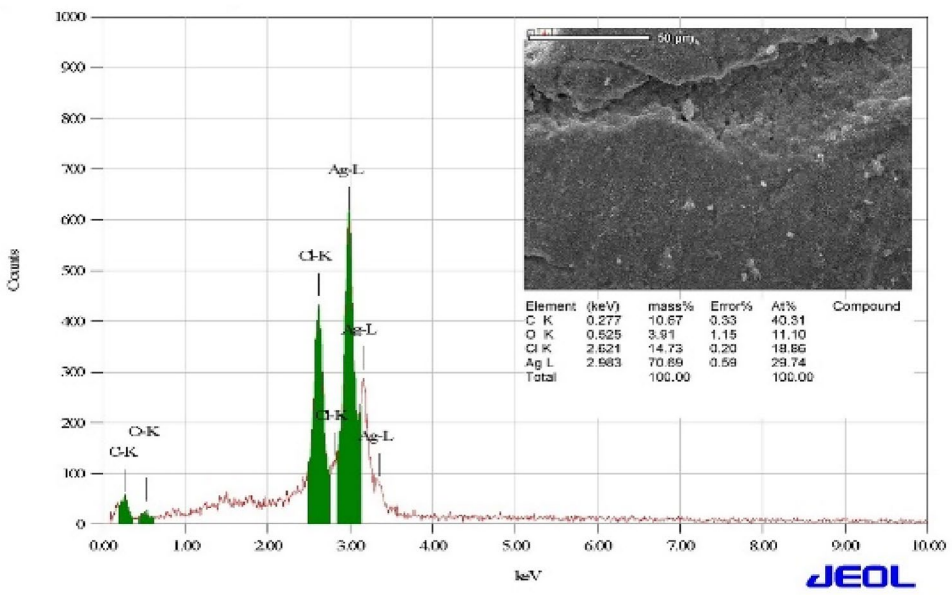

Fig. 6 EDX analysis of AgNPs using *Mentha piperita*: inset shows the corresponding SEM image

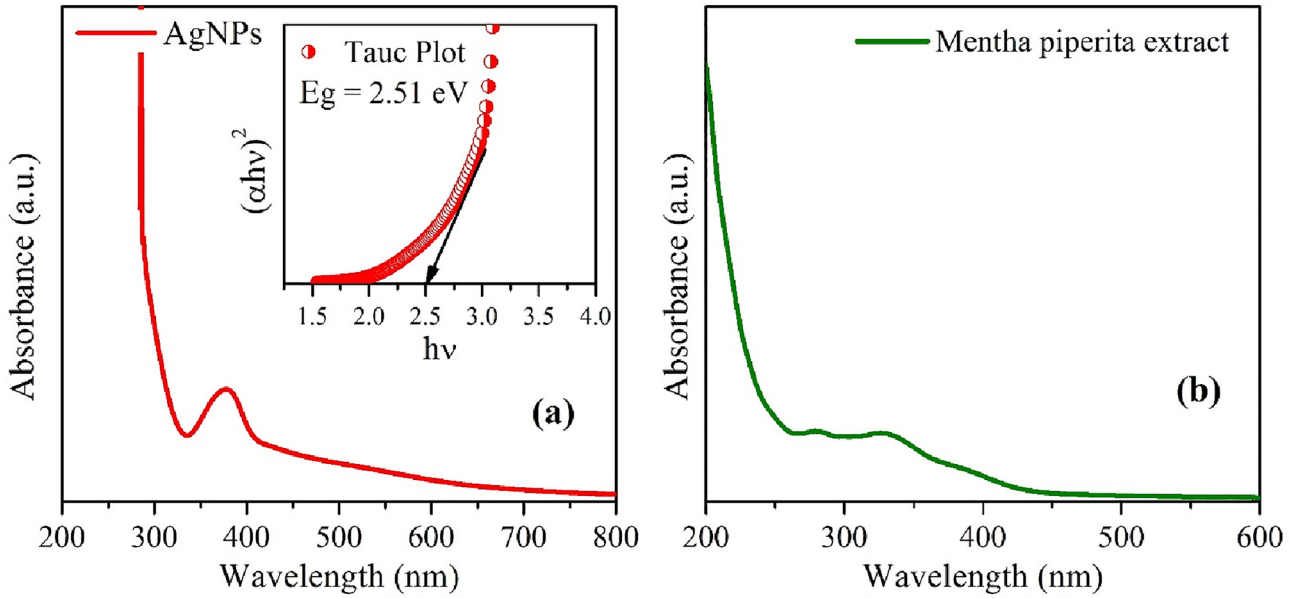

Fig. 7 UV–Vis spectra of AgNPs (**a**): inset shows the Tauc plot for band gap calculation, and UV–Vis absorption spectra of *Mentha piperita* extract (**b**)

at 380 nm. This can be ascribed to the scattering effect from the haphazardly oriented nano-crystallites/grains with grain boundaries (Cai et al. 2017).

The optical band gap E_g of biologically synthesized AgNPs sample is calculated using Tauc plot as derived from the relation (Eq. 4) (Akhter et al. 2020) as shown in the inset of Fig. 7 (a), given by

$$\alpha h\nu = C(h\nu - E_g)^n, \tag{4}$$

where α is the absorption coefficient ($\alpha = \frac{2.303 \times A}{t}$; here, t is the thickness of cuvette (1 cm), and A is the absorbance), C is the energy-independent coefficient, $h\nu$ is the photon energy, and E_g is the optical band gap of the synthesized AgNPs. Further, the value of n is considered ½ as silver NPs have the direct band gap. The optical band gap of AgNPs can be evaluated by the linear extrapolation of the plot of $(\alpha h\nu)^2$ versus $h\nu$ on the x-axis (*i.e.,* $E_g = 2.51\ eV$). This band gap of the sample may be arise because of the least intermediate energy levels and smaller average grain/crystallite size of the AgNPs sample. This characteristic of wide optical band gap of AgNPs substituted its utilization in biomedical applications (Usman et al. 2012).

Antifungal activity of AgNPs

In disc technique, the antifungal effectiveness of AgNPs against all fungi was markedly significant against all strains with 100% (18) as shown in Table 2. Broth microdilution method emphasized and matched the positive results of disc method depending on Minimum effective concentration (MEC) and gave more accurate findings to determine Minimum inhibition concentration (MIC) in which disc method could not cover it as observed in Table 3.

27.8% (5) of isolates were sensitive to the lowest concentration of nanoparticles (25 ppm) especially *A. flavus* (AM4), and *A. niger* (AM17) through disc method in which this percentage increased to 44.4% (8) in broth method especially against *A. flavus* (AM15) and *A. niger* (AM17). MIC, MFC and MEC were 200 ppm in 66.7% (12), 200 ppm in 55.6% (10) and 25 ppm in 44.4% (8) of fungi, respectively.

There are numerous studies focusing on menthe plant either extract, oil, or nanoparticles and its efficiency as antibacterial, antifungal or antioxidant agent. However, there are limited published reports either studying the efficacy of silver nanoparticles of *Mentha piperita* on filamentous fungi, especially against resistance *Aspergillus* species, or studying the evaluation of disc compared to broth microdilution method in nanoparticles application against nanoparticles filamentous fungi. The efficiency of Ag NPs of *Mentha spicata* against *A. niger* of Alkfaji report (Alkfaji et al. 2020) was almost similar to our results, although the concentration of Ag NPs was higher (20 mg) than our concentration (0.025 mg/ml). Abd Kelkawi (2017) studied the susceptibility of *C. albicans* to AgNPs of *Mentha pulegium* and recorded 100 ppm as MIC which was similar to our result in 11.1% (2) of fungi: *A. niger* (AM17) and *A. flavous* (AM15) (Abd Kelkawi et al. 2017). Moreover, MIC, MFC, and MEC of Au NPs of *Mentha piperita* in our previous report (Almansob et al. 2022) were 1000 ppm in 20% (1),

Table 3 Efficacy of different concentrations of AgNPs of *Mentha piperita* against susceptible fungi with disc method (Broth microdilution technique)

NO	Fungi	Growth rate (scores/4)				
		AgNPs				
		25	50	100	200	1000
1	*A. flavus (AM1)*	4±0	4±0	3±0*	0±0**^{F}	0±0
2	*A. flavus (AM2)*	4±0	4±0	3±0*	0±0**^{F}	0±0
3	*A. flavus (AM3)*	3±0*	2±0	1±0	0±0** ^{F}	0±0
4	A. *flavus (AM4)*	4±0	4±0	3±0*	0±0** ^{F}	0±0
5	A. *flavus (AM5)*	3±0*	2±0	1±0	0±0** ^{F}	0±0
6	*A. fumigatus (AM6)*	4±0	3±0*	2±0	0±0** ^{F}	0±0
7	A. *fumigatus(AM7)*	4±0	4±0	3±0*	0±0**	0±0 ^{F}
8	A. *niger (AM8)*	3±0*	0±0**	0±0 ^{F}	0±0	0±0
9	*A. niger (AM9)*	3±0*	0±0** ^{F}	0±0	0±0	0±0
10	*A. terreus (AM10)*	4±0	4±0	3±0*	2±0	0±0** ^{F}
11	A. *flavus (AM11)*	4±0	3±0*	1±0	0±0** ^{F}	0±0
12	A.*flavus (AM12)*	3±0*	2±0	1±0	0±0** ^{F}	0±0
13	A. *flavus (AM13)*	4±0	2±0*	1±0	0±0**	0±0 ^{F}
14	*A. terreus 8*	4±0	3±0*	1±0	0±0** ^{F}	0±0
15	A. *flavus (AM14)*	4±0	1±0*	0±0** ^{F}	0±0	0±0
16	A. *flavus (AM15)*	0±0*** ^{F}	0±0	0±0	0±0	0±0
17	*A. flavus (AM16)*	3±0*	2±0	1±0	0±0** ^{F}	0±0
18	A. *niger (AM17)*	4±0	4±0	3±0*	0±0**^{F}	0±0

*MEC, **MIC, ***MEC&MIC& ^{F}M

1000 ppm in 20% (1), and 60% (3) of fungi, respectively, indicating the effectiveness of Au NPs in higher concentration compared to AgNPs which was more efficient in a small amount.

In general, differences in the efficacy of the nanoparticles may attribute to size, shape, concentration, and types of nanoparticles such as nanoparticles with small sizes have the capability to enter cells and interact with significant internal components (Karlsson et al. 2009; Sanghi and Verma 2009; Abbaszadegan et al. 2015; Abdelmonem et al. 2015; Zhao et al. 2015), and this was recorded in our finding in which silver nanoparticles of *M. piperita* were smaller (Av:30 nm) with spherical shapes. Overall, Tafrihi et al. (Tafrihi et al. 2021) showed wonderful activities of *Mentha* sp. in various reports, and this is convenient to our finding as nanoparticles form as interesting and promised antifungal efficacy.

Effect of silver nanoparticles on extracellular fungal enzymes activity

As shown in Fig. 8, nineteen extracellular enzymes profiling of *A. fumigatus* (AM6) was studied. High concentrations of enzymatic activity (20–30 nmoles) were recorded only in 10.5% (2), which were Naphthol-AS-BI-phosphohydrolase and alkaline phosphatase, low to moderate amount (5–10 nmoles) noted in 15.8% (3) and there was no enzymatic activity in 73.7% (14) of enzymes. Enzymes profiling was notably modified after treatment fungus with AgNPs in which all enzymatic changes 89.5% (17) significantly increased especially α-chymotrypsin, ß-glucuronidase, ß-glucosidase and N-acetyl-ß-glucosaminidase.

The accurate mechanisms of Ag NPs capacity in inhibition filamentous fungi especially *Aspergillus* are challenging. Therefore, there are few published reports focusing on this area. The mechanisms of effect may have attributed to one or more factors either on molecular or physiological levels such as cell wall degradation and change enzymes activity (Feng et al. 2000; Du et al. 2020; Ameen et al. 2021). In our study, Ag NPs increased most of enzymatic activity which agree with Pietrzak (2015) report recorded against *A. niger* with another source of AgNPs (Pietrzak et al. 2015). Nevertheless, the highest increases enzymes were α-chymotrypsin, ß-glucuronidase, ß-glucosidase and N-acetyl-ß-glucosaminidase different from our report which indicate the change may be attributed to type of fungus and/or type of adding agents (Gutarowska 2010). However, impact of Au NPs against *A. flavus* in our previous report (Almansob et al. 2022) was in the opposite face of Ag NPs in which increased enzymatic activity of eleven enzymes observed with Ag NPs effect decreased with Au NPs influence especially acid phosphatase, α-galactosidase, ß-glucosidase and N-acetyl-ß-glucosaminidase. Moreover, α-galactosidase and ß-glucosidase are the crucial significant modification of enzymatic activity between Ag NPs

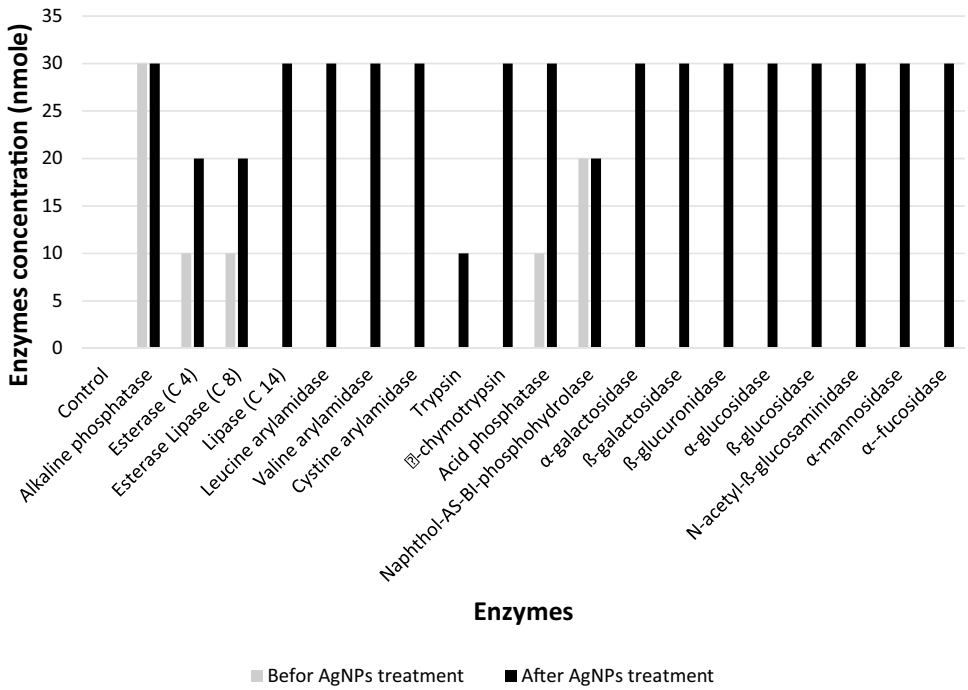

Fig. 8 Efficacy of AgNPs on extracellular enzymes activity of *A. fumigatus* (AM6)

and Au NPs in which these enzymes increased (from 0 to 30 nmoles) due to influence former and highly eliminated (from 30 to 0 nmoles) as an impact of latter. ß-galactosidase, ß-glucuronidase and α-glucosidase are interesting enzymes, the activity of which increased as a result of effect of both Ag NPs and Au NPs against different fungi species. However, this observation is inconsistent with Pietrzak (2015) reporting decrease in α-glucosidase activity in *Penicillium chrysogenum* treated with different type of Ag NPs (Pietrzak et al. 2015).

Conclusion

The extract of *Mentha piperita* was utilized to produce green synthesized silver nanoparticles, biologically and characterized using various techniques. XRD, HRTEM, SAED, FT-IR and Raman analysis confirm the absence of any additional phases in the sample, resulting the pure fcc single-phase structure of Ag NPs. The average crystallite (grain) size is found to be ~ 22 nm, and average particle size of the samples is measured as ~ 30 nm from TEM, while the optical band gap stays around ~ 2.51 eV. EDX spectrum confirms the phase purity and presence of Ag and O elements in the sample. Additionally, there are limited studies published in Saudi Arabia focusing on resistant *Aspergillus* and the worsening threat. Hence, the biosynthesized Ag NPs can be applied for the coating of medical appliances to control the nosocomial fungal infections and also be a promising candidate for safeguarding the health of patients.

Acknowledgements This research was funded by Researchers Supporting Project number (RSP-2021/364), King Saud University, Riyadh, Saudi Arabia.

Declarations

Conflict of interest The authors declare that they have no conflict of interest.

References

Abbaszadegan A, Ghahramani Y, Gholami A, et al (2015) The effect of charge at the surface of silver nanoparticles on antimicrobial activity against gram-positive and gram-negative bacteria: a preliminary study. J Nanomaterials 2015:

Abd Kelkawi AH, Kajani AA, Bordbar AK (2017) Green synthesis of silver nanoparticles using *Mentha pulegium* and investigation of their antibacterial, antifungal and anticancer activity. IET Nanobiotechnol 11:370–376. https://doi.org/10.1049/iet-nbt.2016.0103

Abdelmonem AM, Pelaz B, Kantner K et al (2015) Charge and agglomeration dependent in vitro uptake and cytotoxicity of zinc oxide nanoparticles. J Inorg Biochem 153:334–338

Abdul M, Khan M, Kumar S, et al (2011) Structural and thermal studies of silver nanoparticles and electrical transport study of their thin films. 1–8

Akhter G, Khan A, Ali SG et al (2020) Antibacterial and nematicidal properties of biosynthesized Cu nanoparticles using extract of holoparasitic plant. SN Appl Sci 2:1–6

Alkfaji F, Today IH-DI (2020) undefined (2020) Biosynthesis of silver nanoparticles with *Mentha spicata* against *Aspergillus niger*. SearchEbscohostCom 14:806–811

Almahdi H, Malik S, Joseph M et al (2016) Fungal infections in aseer central hospital: a retrospective laboratory-based study of 340

cases during the years 2011 to 2015. Br J Med Med Res 12:1–8. https://doi.org/10.9734/bjmmr/2016/22650
Almansob A, Bahkali AH, Ameen F (2022) Efficacy of gold nanoparticles against drug-resistant nosocomial fungal pathogens and their extracellular enzymes : resistance profiling towards established antifungal agents
Almuneef MA, Memish ZA, Balkhy HH et al (2006) Rate, risk factors and outcomes of catheter-related bloodstream infection in a paediatric intensive care unit in Saudi Arabia. J Hosp Infect 62:207–213. https://doi.org/10.1016/j.jhin.2005.06.032
Al-Tawfiq JA, Abed MS (2009) Prevalence and antimicrobial resistance of health care associated bloodstream infections at a general hospital in Saudi Arabia. Saudi Med J 30:1213–1218
Ameen F (2022) Optimization of the synthesis of fungus-mediated bi-metallic Ag-Cu nanoparticles. Appl Sci 12:1384
Ameen F, AlYahya S, Govarthanan M, et al (2020) Soil bacteria *Cupriavidus* sp. mediates the extracellular synthesis of antibacterial silver nanoparticles. J Mol Struct 1202:127233
Ameen F, Alsamhary K, Alabdullatif JA, ALNadhari S (2021) A review on metal-based nanoparticles and their toxicity to beneficial soil bacteria and fungi. Ecotoxicology and Environmental Safety 213:112027
Ameen F, Al-Maary KS, Almansob A, AlNadhari S (2022) Antioxidant, antibacterial and anticancer efficacy of *Alternaria chlamydospora*-mediated gold nanoparticles. Applied Nanoscience 1–8
Arendrup MC (2014) Update on antifungal resistance in *Aspergillus* and *Candida*. Clin Microbiol Infect 20:42–48
Arvizo RR, Bhattacharyya S, Kudgus RA et al (2012) Intrinsic therapeutic applications of noble metal nanoparticles: past, present and future. Chem Soc Rev 41:2943. https://doi.org/10.1039/c2cs15355f
Cai Y, Piao X, Gao W et al (2017) Large-scale and facile synthesis of silver nanoparticles: Via a microwave method for a conductive pen. RSC Adv 7:34041–34048. https://doi.org/10.1039/c7ra05125e
Desam NR, Al-Rajab AJ, Sharma M et al (2019) Chemical constituents, in vitro antibacterial and antifungal activity of Mentha × Piperita L. (peppermint) essential oils. J King Saud Univ Sci 31:528–533. https://doi.org/10.1016/j.jksus.2017.07.013
Du J, Zhang Y, Yin Y et al (2020) Do environmental concentrations of zinc oxide nanoparticle pose ecotoxicological risk to aquatic fungi associated with leaf litter decomposition? Water Res 178:115840
Ebrahimabadi AH, Ebrahimabadi EH, Djafari-Bidgoli Z et al (2010) Composition and antioxidant and antimicrobial activity of the essential oil and extracts of Stachys inflata Benth from Iran. Food Chem 119:452–458
Feng QL, Wu J, Chen GQ et al (2000) A mechanistic study of the antibacterial effect of silver ions on *Escherichia coli* and *Staphylococcus aureus*. J Biomed Mater Res 52:662–668
Feng L, Zhang C, Gao G, Cui D (2012) Facile synthesis of hollow Cu_2O octahedral and spherical nanocrystals and their morphology- dependent photocatalytic properties. 1–10
Gabriela Á-M, Gabriela M de O-V, Luis A-M et al (2017) Biosynthesis of silver nanoparticles using mint leaf extract (*Mentha piperita*) and their antibacterial activity. Adv Sci Eng Med 9:914–923. https://doi.org/10.1166/asem.2017.2076
Gnat S, Łagowski D, Nowakiewicz A, Dyląg M (2021) A global view on fungal infections in humans and animals: opportunistic infections and microsporidioses. J Appl Microbiol. https://doi.org/10.1111/jam.15032
Gutarowska B (2010) Metabolic activity of moulds as a factor of building materials biodegradation. Pol J Microbiol 59:119
Gutarowska B, Pietrzak K, Machnowski W et al (2014) Application of silver nanoparticles for disinfection of materials to protect historical objects. Curr Nanosci 10:277–286
Habibi MH, Kamrani R, Mokhtari R (2010) Fabrication and characterization of copper nanoparticles using thermal reduction: the effect of nonionic surfactants on size and yield of nanoparticles. Microchim Acta 171:91–95. https://doi.org/10.1007/s00604-010-0413-2
Inbathamizh L, Ponnu TM, Mary EJ (2013) In vitro evaluation of antioxidant and anticancer potential of *Morinda pubescens* synthesized silver nanoparticles. J Pharm Res 6:32–38
Jadhav K, Dhamecha D, Bhattacharya D, Patil M (2016) Green and ecofriendly synthesis of silver nanoparticles: characterization, biocompatibility studies and gel formulation for treatment of infections in burns. J Photochem Photobiol, B 155:109–115
Jafarizad A, Safaee K, Gharibian S et al (2015) Biosynthesis and in-vitro study of gold nanoparticles using mentha and pelargonium extracts. Proc Materials Sci 11:224–230. https://doi.org/10.1016/j.mspro.2015.11.113
Jha AK, Prasad K, Prasad K, Kulkarni AR (2009) Plant system: nature's nanofactory. Colloids Surf, B 73:219–223
Joshi N, Jain N, Pathak A et al (2018) Biosynthesis of silver nanoparticles using *Carissa carandas* berries and its potential antibacterial activities. J Sol-Gel Sci Technol 86:682–689. https://doi.org/10.1007/s10971-018-4666-2
Karlsson HL, Gustafsson J, Cronholm P, Möller L (2009) Size-dependent toxicity of metal oxide particles—a comparison between nano- and micrometer size. Toxicol Lett 188:112–118
Khan A, Rashid A, Younas R, Chong R (2016) A chemical reduction approach to the synthesis of copper nanoparticles. Int Nano Lett 6:21–26. https://doi.org/10.1007/s40089-015-0163-6
Khan A, Ameen F, Khan F et al (2020a) Fabrication and antibacterial activity of nanoenhanced conjugate of silver (I) oxide with graphene oxide. Materials Today Communications 25:101667. https://doi.org/10.1016/j.mtcomm.2020.101667
Khan A, Rahman F, Nongjai R, Asokan K (2020b) Structural, optical and electrical transport properties of Sn Doped In 2O3. Solid State Sci 109:106436. https://doi.org/10.1016/j.solidstatesciences.2020.106436
Khan A, Rahman F (2019) Study of microstructural and optical properties of nanocrystalline indium oxide : A transparent conducting oxide (TCO) Study of Microstructural and Optical Properties of Nanocrystalline Indium Oxide : A Transparent Conducting Oxide (TCO). 030091:1–5. https://doi.org/10.1063/1.5112930
Kim D-Y, Saratale RG, Shinde S et al (2018) Green synthesis of silver nanoparticles using *Laminaria japonica* extract: characterization and seedling growth assessment. J Clean Prod 172:2910–2918. https://doi.org/10.1016/j.jclepro.2017.11.123
Linic S, Aslam U, Boerigter C, Morabito M (2015) Photochemical transformations on plasmonic metal nanoparticles. Nat Mater 14:567–576. https://doi.org/10.1038/nmat4281
Maddy AJ, Sanchez N, Shukla BS, Maderal AD (2019) Dermatological manifestations of fungal infection in patients with febrile neutropaenia: a review of the literature. Mycoses 62:826–834
MubarakAli D, Thajuddin N, Jeganathan K, Gunasekaran M (2011) Plant extract mediated synthesis of silver and gold nanoparticles and its antibacterial activity against clinically isolated pathogens. Colloids Surf, B 85:360–365. https://doi.org/10.1016/j.colsurfb.2011.03.009
Murugesan S, Bhuvaneswari S, Sivamurugan V (2017) Green synthesis, characterization of silver nanoparticles of a marine red alga *spyridia fusiformis* and their antibacterial activity. Int J Pharmacy Pharmaceut Sci 9:192. https://doi.org/10.22159/ijpps.2017v9i5.17105
Parlinska-Wojtan M, Kus-Liskiewicz M, Depciuch J, Sadik O (2016) Green synthesis and antibacterial effects of aqueous colloidal solutions of silver nanoparticles using camomile terpenoids as a combined reducing and capping agent. Bioprocess Biosyst Eng 39:1213–1223

Pietrzak K, Twarużek M, Czyżowska A, et al (2015) Influence of silver nanoparticles on metabolism and toxicity of moulds. Acta Biochimica Polonica 62:

Rajadurai UM, Hariharan A, Durairaj S et al (2021) Assessment of behavioral changes and antitumor effects of silver nanoparticles synthesized using diosgenin in mice model. J Drug Delivery Sci Technol 66:102766

Rajkumar A, Sivarajasekar N, Kandasamy S (2021) Bio-synthesized silver nanoparticles for effective photo-catalytic degradation of congo red dye in aqueous solutions: optimization studies using response surface methodology. Anal Chem Lett 11:801–815

Roselina NRN, Azizan A (2012) Ni nanoparticles: study of particles formation and agglomeration. Proc Eng 41:1620–1626. https://doi.org/10.1016/j.proeng.2012.07.359

Rudramurthy SM, Paul RA, Chakrabarti A et al (2019) Invasive aspergillosis by *Aspergillus flavus*: epidemiology, diagnosis, antifungal resistance, and management. J Fungi 5:1–23. https://doi.org/10.3390/jof5030055

Sajjad S, Arshad F, Uzair B et al (2019) GO/Ag_2O composite nanostructure as an effective antibacterial agent. Chem Select 4:10365–10371. https://doi.org/10.1002/slct.201902641

Sanghi R, Verma P (2009) Biomimetic synthesis and characterisation of protein capped silver nanoparticles. Biores Technol 100:501–504

Sathishkumar P, Preethi J, Vijayan R et al (2016a) Anti-acne, anti-dandruff and anti-breast cancer efficacy of green synthesised silver nanoparticles using *Coriandrum sativum* leaf extract. J Photochem Photobiol, B 163:69–76

Sathishkumar P, Vennila K, Jayakumar R et al (2016b) Phytosynthesis of silver nanoparticles using *Alternanthera tenella* leaf extract: an effective inhibitor for the migration of human breast adenocarcinoma (MCF-7) cells. Bioprocess Biosyst Eng 39:651–659

Siddiqi KS, Husen A, Rao RAK (2018) A review on biosynthesis of silver nanoparticles and their biocidal properties. J of Nanobiotechnol 16:. https://doi.org/10.1186/s12951-018-0334-5

Song G, Liang G, Liu W (2020) Fungal co-infections associated with global COVID-19 pandemic: a clinical and diagnostic perspective from China. Mycopathologia 185:599–606. https://doi.org/10.1007/s11046-020-00462-9

Sreelatha S, Padma PR, Umadevi M (2009) Protective effects of *coriandrum sativum* extracts on carbon tetrachloride-induced hepatotoxicity in rats. Food Chem Toxicol 47:702–708

Tafrihi M, Imran M, Tufail T et al (2021) The wonderful activities of the genus *Mentha*: Not only antioxidant properties. Molecules 26:1–22. https://doi.org/10.3390/molecules26041118

Thirunavoukkarasu M, Balaji U, Behera S et al (2013) Biosynthesis of silver nanoparticle from leaf extract of *Desmodiumgangeticum* (L.) DC. and its biomedical potential. Spectrochim Acta Part A Mol Biomol Spectrosc 116:424–427. https://doi.org/10.1016/j.saa.2013.07.033

Usman MS, Ibrahim NA, Shameli K et al (2012) Copper nanoparticles mediated by chitosan: synthesis and characterization via chemical methods. Molecules 17:14928–14936. https://doi.org/10.3390/molecules171214928

Zhao X, Lu D, Hao F, Liu R (2015) Exploring the diameter and surface dependent conformational changes in carbon nanotube-protein corona and the related cytotoxicity. J Hazard Mater 292:98–107